AIP Conference Proceedings

Nuclear structure of some even and odd nuclei using shell model calculations

Cite as: AIP Conference Proceedings **2292**, 030002 (2020); https://doi.org/10.1063/5.0030932
Published Online: 27 October 2020

Bhopendra Singh, S. Suman Rajest, K. Praghash, Uppalapati, and Srilakshmi R. Regin

View Online Export Citation

ARTICLES YOU MAY BE INTERESTED IN

Shadowing and non-shadowing in dynamical systems
AIP Conference Proceedings **2292**, 020012 (2020); https://doi.org/10.1063/5.0030805

Inverse shadowing property of transitivity with G-and topological G
AIP Conference Proceedings **2292**, 020013 (2020); https://doi.org/10.1063/5.0031013

Two-phase relative permeability prediction from capillary pressure data for one Iraqi oil field: A comparative study
AIP Conference Proceedings **2292**, 030001 (2020); https://doi.org/10.1063/5.0030501

Meet the Next Generation of Quantum Analyzers
And Join the Launch Event on November 17th

Register now
Zurich Instruments

© 2020 Author(s).

Nuclear Structure of Some Even and Odd Nuclei Using Shell Model Calculations

Bhopendra Singh[1,a)] S. SumanRajest [2.b)] K. Praghash [3,c)]
Uppalapati[4,d)] and Srilakshmi R.Regin[5,e)]

[1]*Associate Professor, Amity University, Dubai.*
[2] *Reacher, Vels Institute of Science, Technology & Advanced Studies (VISTAS), Chennai, Tamil Nadu, India.*
[3]*Assistant Professor, Koneru Lakshmaiah Education Foundation, Vaddeswaram, AP, India.*
[4]*Assistant Professor, CSE Department, VFSTR Deemed to be University, Vadlamudi, Guntur, India.*
[5]*Assistant professor, Adhiyamaan College of Engineering, Hosur, Tamil Nadu, India.*

Corresponding Author:-[a)] bsingh@amityuniversity.ae
[b)] sumanrajest414@gmail.com
[c)]prakashcospra@gmail.com
[d)]druppalapati2019@gmail.com
[e)]regin12006@yahoo.co.in

Abstract: In this work, we determined the electron dispersing structure factors, just as the vitality levels of certain cores. The computation of electron dispersing structure factors needs numerous issues to be remembered for request to make these figures attainable and quick in time in light of enormous measure of terms speak to arithmetic, quantum mechanical speculations, atomic shell model hypotheses and equations. In the current work, we examined the impacts of the higher setup outside the shell model space and the inactive center which included Tassie Model (TM) to discuss the Longitudinal C2 electron scattering form factors for the nuclei: ^{116}Sn, ^{92}Mo,^{90}Zr ,^{39}K and ^{32}S, which calculated for nuclei under consideration, are compared with those of experimental data. The HO and SKX possibilities have been utilized to compute the wave elements of outspread single-molecule framework components. Some hypothetical vitality levels of the ^{52}Cr, ^{32}S and ^{181}Ta nuclei are calculated compared with their experimental data. The shell model for windows code NuShellX@MSU has been used in this study.

INTRODUCTION

The atomic Shell model gives the significant hypothetical apparatus to understanding the atomic properties. It very well may be utilized in the least complex types of individual particles to give a subjective origination, yet it is likewise utilized as a reason for substantially more intricate and complete estimations. There has all the earmarks of being constrained inside the not so distant future to the extension of its application [1]. The scattering of electrons from the nuclei provides important information about the electromagnetic currents inside the nuclei. Electronic scattering can provide a good tool for this calculation because it is sensitive to the locative dependence of the current and charge density [2, 3]. Important information about the nuclear structure can be obtained by the scattering of electrons at high energy. Information obtained at high-energy electron scattering depends on the wavelength of the de Broglie wavelength associated with the electron compared to the range of nuclear forces. If the incident electron energy is 100 MeV and more, the de Broglie wavelength will be in the spatial extent of the target nucleus [23-27]. Thus , the electron with these energies is the best probe for studying the nuclear structure [4]. Electron scattering is the most important tool to study the nuclear structure for many reasons, the electron and nucleus interaction is well known as the electron interacts electromagnetically with the local charge and the current and magnetic density of

Proceedings of the 2020 2nd International Conference on Sustainable Manufacturing, Materials and Technologies
AIP Conf. Proc. 2292, 030002-1–030002-7; https://doi.org/10.1063/5.0030932
Published by AIP Publishing. 978-0-7354-4024-1/$30.00

the nucleus. measurements can be obtained without significantly impairing the structure of target nuclei. While in the case of scattering of a nucleon from nuclei, neither the interaction nor the structure of the target is well known therefore it is very complicated to distinguish between them by analyzing the experimental data [28-36]. With electron scattering One can instantly connect the cross section with the transition matrix elements of the operators of local charge and current density and consequently directly related to the nuclear structure of the target itself [5, 6]. In electron scattering, one can distinguish two types of scattering: first the nucleus is left on its ground state; this process is called "Elastic Electron Scattering". In the second type, the nucleus is left in its different excited states, this process is called " Inelastic Electron Scattering" [7].

Inelastic Longitudinal Form Factors

Inelastic form factors involving angular momentum J and momentum transfer q can be written in terms of the elements of the reduced matrix in both angular momentum and isospin [8].

$$\left|F_J^L(q)\right|^2 = \frac{4\pi}{Z^2(2J_i+1)}\left|\sum_{T=0,1}(-1)^{T_f-T_{z_f}}\begin{pmatrix} T_f & T & T_i \\ -T_{Z_f} & 0 & T_{Z_i}\end{pmatrix}\left\langle f \left\| \hat{T}^L_{JT}(q) \right\| i\right\rangle\right|^2$$

$$\left|F_{cm}(q)\right|^2 \left|F_{fs}(q)\right|^2 \tag{1}$$

The diminished grid components of the longitudinal administrator in the turn and isospin space are given between conditions of the last and starting numerous particles of the framework remembering the setup blend for terms of OBDM components increased by the single molecule lattice components of the longitudinal operator [9],

$$\text{i.e.}\left\langle f \left\| \hat{T}^L_{JT} \right\| i \right\rangle = \sum_{a,b} OBDM^{JT}(i,f,J,a,b)\left\langle b \left\| \hat{T}^L_{JT} \right\| a \right\rangle \tag{2}$$

The OBDM elements are given in terms of the isospin reduced matrix elements [10], i.e.

$$OBDM(\tau_Z) = (-1)^{T_f - T_z}\begin{pmatrix} T_f & 0 & T_i \\ -T_Z & 0 & T_Z\end{pmatrix}\sqrt{2}\ \frac{OBDM(\Delta T=0)}{2} + \tau_Z(-1)^{T_f - T_z}\begin{pmatrix} T_f & 1 & T_i \\ -T_Z & 0 & T_Z\end{pmatrix}\sqrt{6}\frac{OBDM(\Delta T=1)}{2} \tag{3}$$

where τ_Z are the isospin operators of single particle. The OBDM(ΔT) is defined [10] as :

$$OBDM(i,f,j,j',\Delta T) = \frac{\left\langle f \left\| \left[a_j^+ \times \tilde{a}_{j'}\right]^{J,\Delta T} \right\| i\right\rangle}{\sqrt{2J+1}\ \sqrt{2\Delta T+1}} \tag{5}$$

The operator a_j^+ creates a nucleon in the single nucleon state j and the operator $\tilde{a}_{j'}$ annihilates a nucleon in the state j'.

Tassie Model (TM) has been utilized to describe the progress of gamma-and the excitation of cores by electron dissipating. As indicated by the aggregate modes, the center polarization change thickness is given by the Tassie shape [11].

$$\rho^{core}_{Jt_z}(i,f,\mathrm{r}) = \mathrm{N}\frac{1}{2}(1+\tau_z)\,\mathrm{r}^{J-1}\frac{d\rho_o(i,f,\mathrm{r})}{d\mathrm{r}} \tag{4}$$

Where N is proportionality constant and ρ_o is the ground state two – body charge density distribution. The Coulomb form factor for this model becomes

$$F_J^L(q) = \left(\frac{4\pi}{2J_i+1}\right)^{1/2}\frac{1}{Z}\left\{\int_0^\infty \mathrm{r}^2 j_J(q\mathrm{r})\rho^{ms}_{Jt_z}\,d\mathrm{r} - \mathrm{N}q\int_0^\infty d\mathrm{r}\,\mathrm{r}^{J+1}\rho_o(i,f,r)\,j_{J-1}(q\mathrm{r})\right\}\times F_{cm}(q)\,F_{fs}(q) \tag{5}$$

The proportionality constant N can be determined from the form factor evaluated at $q=k$, we obtain

$$\mathrm{N} = \frac{\int_0^\infty d\mathrm{r}\, \mathrm{r}^2\, j_J(k\mathrm{r})\, \rho_{Jt_Z}^{ms}(i,f,\mathrm{r}) - F_J^L(k)\, Z\sqrt{\frac{2J_i+1}{4\pi}}}{k\int_0^\infty d\mathrm{r}\, \mathrm{r}^{J+1}\, \rho_o(i,f,\mathrm{r})\, j_{J-1}(k\mathrm{r})} \tag{6}$$

RESULTS, DISCUSSION AND CONCLUSIONS

Energy levels

Some theoretical energy levels of the ^{52}Cr nucleus compared with the experimental data [12] are shown in figure1. The levels are calculated with FPPN model space and gxlpn as two- body interaction. The active orbitals for FPPN model space are P: 1f7/2, 2p3/2,1f5/2, 2p1/2 and N: 1f7/2, 2p3/2, 1f5/2, 2p1/2. Great understanding was gotten for the utilized cooperation. The understanding is generally excellent for most states as contrasted and the trial information. The supreme contrasts among hypothetical and exploratory qualities are nearly between 0.040MeV and 0.4 MeV. Figure 2 Show same comparison for the excited energy levels of ^{32}S nucleus [37-46]. The hasp interaction [13] has been used. The HASP model space defined by the orbitals 1d3/2,2s1/2,2p3/2,1f7/2. This model includes configuration mixing between 1d3/2,2s1/2 of SD model space and 2p3/2,1f7/2 of FP model space. There are reasonable agreement between theoretical and experimental levels [14] for most states. The energy levels of ^{92}Mo nucleus (fig.3) give good agreement compared with the experimental levels [15]. The calculations performed with the N50J Model Space (2P3/2,1F5/2,2p1/2,1g9/2). The calculations of the ^{39}K energy levels (figs. 1 to 4) using hasp interaction give very poor agreement with the experimental data [16].

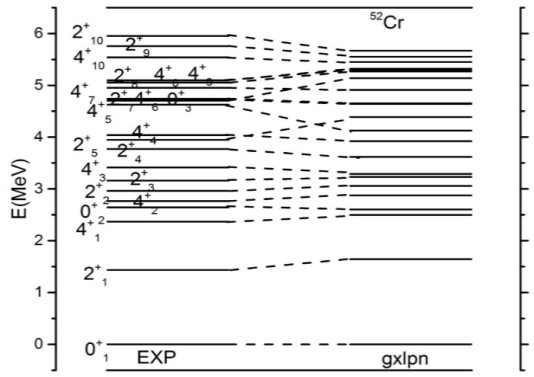

FIGURE 1. Excitation energies for the ^{52}Cr with their corresponding experimental values [12]

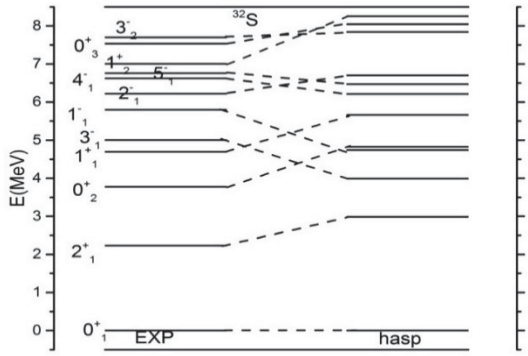

FIGURE 2. Excitation energies for the ^{32}S nuclei compared with experimental values [14]

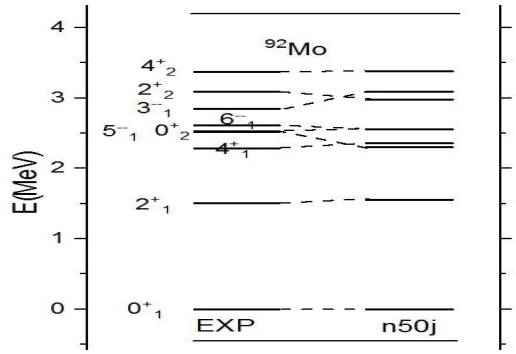

FIGURE 3. Excitation energies for the ^{92}Mo nuclei compared with experimental values [15]

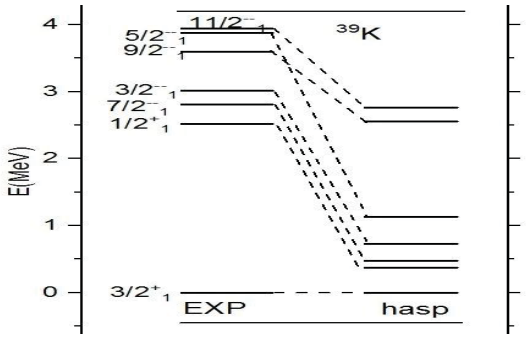

FIGURE 4. Excitation energies for the ^{39}K nuclei with experimental values[16]

Table 1. shows some of the energy levels of ^{181}Ta. The levels are calculated with PBPOP model space, with restrict protons to contribute in 2d5/2, 2d3/2,3s1/2 and 1h9/2 shells, and the neutrons contributed in 2f5/2,3p3/2 and 3p1/2 shells. The interaction failed to expect the ground state, the theoretical ground state J^{π} is $9/2^{-}$, while it is $7/2^{+}$ in the experimental data. Many of other states give poor agreement with the experimental data [17]. There is a computational difficult to calculate the levels with another model space.

Table 1. Excitation energies for the ^{181}Ta nuclei with their corresponding experimental values [17]

^{181}Ta	Ex(MeV)	
J^{π}_{order}	EXP	pbpop
$7/2^{+}_{1}$	0	
$9/2^{-}_{1}$	0.006	0
$7/2^{-}_{1}$	0.7729	0.176
$5/2^{-}_{1}$	0.542	0.298
$13/2^{-}_{1}$	0.337	0.364
$11/2^{-}_{1}$	0.158	0.397
$3/2^{-}_{1}$	—	0.504
$15/2^{-}_{1}$	0.542	0.603
$17/2^{-}_{1}$	0.772	0.748
$1/2^{-}_{1}$	—	0.776
$21/2^{-}_{1}$	1.307	0.983
$19/2^{-}_{1}$	1.027	1.198
$25/2^{-}_{1}$	1.932	1.466
$23/2^{-}_{1}$	1.608	1.469

LONGITUDINAL ELECTRON SCATTERING FORM FACTORS

We have been determined C2 segments of the electron dispersing structure factors for the ^{116}Sn, ^{92}Mo,^{90}Zr ,^{39}K and ^{32}S cores. The HO and SKX (X=20) possibilities have been utilized to figure the wave elements of outspread single-molecule framework components. Fig. 5, shows the figuring of the longitudinal C2 (2^{+}_{1} 2) inelastic electron dispersing structure elements of ^{116}Sn core. The powerful charges that utilized is 0.5 for every one of protons and neutrons. The computations are lower than trial result by a factor of around 3 at the primary greatest and around 4 at the subsequent most extreme. The counts are performed by GLEKPN [18] Model Space (P: 1F7/2,1F5/2, 2P3/2,2P1/2,1G9/2 and N:1G9/2,1G7/2,2D5/2, 2D3/2,3S1/2), and glekpn as two body cooperation. The vitality levels of ^{116}Sn (not appeared) give poor concurrence with the trial information, as model the energies of 2^{+}_{1}and4^{+}_{1} states in hypothetical figures are 1.167MeV and 1.555MeV, separately, while it is 1.294MeV and 2.391MeV in test information. The inelastic longitudinal structure factors for the C2 (2^{+}_{1} 4) state in the 92Mo core is introduced in Fig. 6. In this figure, Calculations of the Tassie model with HO (strong bend) and SKX (ran bend) possibilities give a decent concurrence with the trial information at the main most extreme when we utilize compelling charges (0.5). The two possibilities give poor understanding at the subsequent most extreme. The figures are performed by n50j

model space [19]. Figure 7, shows the estimations of the longitudinal C2 (2_1^+ 5) inelastic electron dispersing structure elements of the ^{90}Zr. The estimations are additionally performed by n50j collaboration. The counts of Tassie Model with HO and SKX give a decent concurrence with the exploratory information at the main most extreme, while the computation with SKX is nearer to the test information at the subsequent greatest. The determined vitality levels (not appeared) utilizing this association give excellent concurrence with test information.

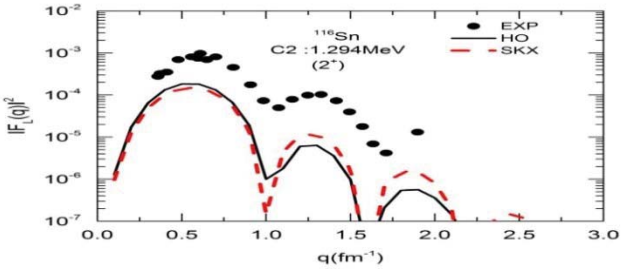

FIGURE 5. The C2 (2_1^+ 2) form factors for the ^{116}Sn nucleus ^{92}Mo nucleus compared with Experimental values [20]

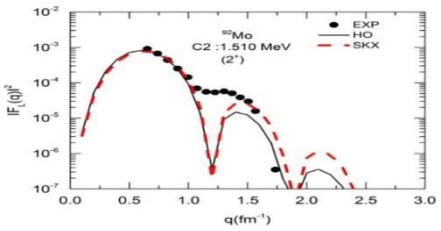

FIGURE 6. The C2 (2_1^+ 4) form factor for the compared with Experimental values [20]

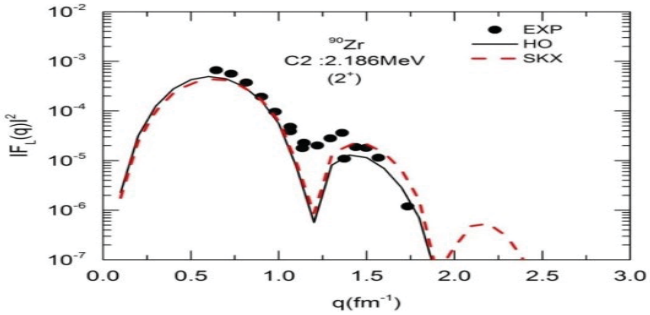

FIGURE 7. The C2 (2_1^+ 5) in ^{90}Zr nucleus compared with Experimental values [20].

The longitudinal C2 ($1/2_1^+$ 1/2) inelastic electron dispersing structure factors in the ^{39}K core is appeared in Fig.8. utilizing the HASP model space. The computations of Tassie model give a decent concurrence with the exploratory information. As appeared in the figure, the computations with SKX are nearer to the exploratory information at the subsequent most extreme. The longitudinal C2 structure factor with center polarization impact (TM) for the

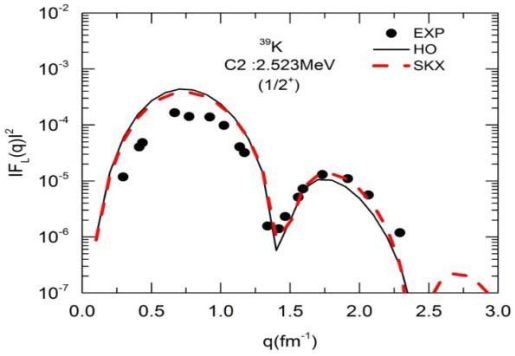

FIGURE 8. The same fig.5 for the ($1/2_1^+$ 1/2) in ^{39}K nucleus. Experimental values [21] are indicated by the filled circles

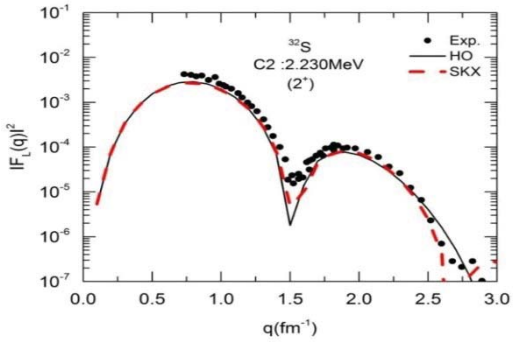

FIGURE 9. The C2 (2_1^+ 0) in ^{32}S nucleus with the Experimental values [22]

transition to the (2_1^+0) in the ^{32}S is appeared in figure 9 contrasted and the trial information. The figuring gauges the test information in the first and the second most extreme area; these estimations with center polarization impact are awesome particularly at the second greatest district and it is commonly worthy. For this situation, the two-body association is hasp. The vitality level computations (Fig.2) are additionally giving adequate concurrence with the information.

CONCLUSION

From this work, it is possible to draw the following conclusions are the theoretical energy levels results with considered effective interaction given a good agreement as compared with experimental data for most states in the ^{52}Cr and ^{32}S nuclei. The HO and SKX potentials are successful to describe the longitudinal form factors for considered nuclei. This study shows obtaining an agreement between theoretical calculations and experimental results of energy levels does not necessarily lead to the same agreement in the calculations of nuclear form factors.

REFERENCES

[1]. B.A. Brown, Towards the future of the nuclear shell model, Nucl. Phys. A, 704, 11 (2002).
[2]. L. Lapikas, A. Dieperink, G. Box, Elastic electron scattering from the magnetization distribution of 27Al, Nucl. Phys. A, 203, 609 (1973).
[3]. J. Bergstrom, S. Kowalski, R. Neuhausen, Elastic magnetic form factor of Li 6, Phys. Rev. C, 25, 1156 (1982).
[4]. R. Roy, B. Nigam, Nuclear Physics Theory and Experiment, John Wiley and Sons, Inc, (1967).
[5]. H. Benson, B. Flowers, A study of deformation in light nuclei:(I). Application to the ground state band of 20Ne and to the low-energy spectrum of 19F, Nucl. Phys. A, 126, 305 (1969).
[6]. J.D. Walecka, Electron scattering for nuclear and nucleon structure, Cambridge University Press (2001).
[7]. D.J. Millener, D. Sober, H. Crannell, J. O'Brien, L. Fagg, S. Kowalski, C. Williamson, L. Lapikas, Inelastic electron scattering from C 13, Phys. Rev. C, 39, 14 (1989).
[8]. T.W. Donnelly, I. Sick, Elastic magnetic electron scattering from nuclei, Rev. of Mod. Phys., 56, 461 (1984).
[9]. P.J. Brussaard, P.W.M. Glaudemans, P. Glaudemans, Shell-model applications in nuclear spectroscopy, North-Holland publishing company (1977).
[10]. B.A. Brown, R. Radhi, B.H. Wildenthal, electric quadrupole and hexadecupole nuclear excitations from the perspective of electron scattering and modern shell-model theory, north-holland publ. co., amsterdam, (1983).
[11]. L. Tassie, A Model of Nuclear Shape Oscillations for g? Transitions and Electron Excitation, Aus. J. of phys., 9, 407 (1956).
[12]. J. Beene, Nuclear data sheets for A= 52, Nuclear Data Sheets, 25, 235 (1978).
[13]. M. Bissell, J. Papuga, H. Naïdja, K. Kreim, K. Blaum, M. De Rydt, R.G. Ruiz, H. Heylen, M. Kowalska, R. Neugart, Proton-Neutron Pairing Correlations in the Self-Conjugate Nucleus K 38 Probed via a Direct Measurement of the Isomer Shift, Phys. rev. lett., 113, 052502 (2014).
[14]. C. Ouellet, B. Singh, Nuclear data sheets for A= 32, Nuclear Data Sheets, 112, 2199 (2011).
[15]. C.M. Baglin, Nuclear data sheets for A= 92, Nuclear Data Sheets, 113, 2187 (2012).
[16]. J. Chen, Nuclear Data Sheets for A= 39, Nuclear Data Sheets, 149, 1 (2018).
[17]. S.-C. Wu, Nuclear data sheets for A= 181, Nuclear Data Sheets, 106, 367 (2005).
[18]. H. Mach, E. Warburton, R. Gill, R. Casten, J. Becker, B. Brown, J. Winger, Meson-exchange enhancement of the first-forbidden Y g 96 (0−)→ 96 Zr g (0+) β transition: β decay of the low-spin isomer of Y 96, Phys. Rev. C, 41, 226 (1990).
[19]. X. Ji, B. Wildenthal, Shell-model calculations for the energy levels of the N= 50 isotones with A= 80–87, Phys. Rev. C, 40, 389 (1989).
[20]. J. Bellicard, P. Leconte, I. Sick, Inelastic electron scattering from even single-closed-shell nuclei, Nucl. Phys. A, 210, 189 (1973).
[21]. H. Sagawa, B. Brown, E2 core polarization for sd-shell single-particle states calculated with a skyrme-type interaction, Nucl. Phys. A, 430, 84 (1984).
[22]. B. Wildenthal, B.A. Brown, I. Sick, Electric hexadecupole transition strength in S 32 and shell-model predictions for E4 systematics in the sd shell, Phys. Rev. C, 32, 2185 (1985).
[23]. Md. Salamun Rashidin, Sara Javed, Bin Liu, Wang Jian, Suman Rajest S "Insights: Rivals Collaboration on Belt and Road Initiatives and Indian Recourses" in Journal of Advanced Research in Dynamical and Control Systems, Vol. 11, SI. 04, Page No.: 1509-1522,2019.
[24]. Loor, Y. del P. C., Cedeno, R. J. P., & Robaina, D. A. (2017). Diagnosis of laboratories of physics and chemistry in the Universidad Tecnica de Manabi. International Research Journal of Management, IT and Social Sciences, vol. 4, no. 4, pp. 1-10, 2017.
[25]. H. Anandakumar and K. Umamaheswari, "An Efficient Optimized Handover in Cognitive Radio Networks using Cooperative Spectrum Sensing," Intelligent Automation & Soft Computing, pp. 1–8, Sep. 2017. doi:10.1080/10798587.2017.1364931

[26]. Haldorai and A. Ramu, "An Intelligent-Based Wavelet Classifier for Accurate Prediction of Breast Cancer," Intelligent Multidimensional Data and Image Processing, pp. 306–319.
[27]. M. Suganya and H. Anandakumar, "Handover based spectrum allocation in cognitive radio networks," 2013 International Conference on Green Computing, Communication and Conservation of Energy (ICGCE), Dec. 2013.doi:10.1109/icgce.2013.6823431. doi:10.4018/978-1-5225-5246-8.ch012
[28]. S, D., & H, A. (2019). AODV Route Discovery and Route Maintenance in MANETs. 2019 5th International Conference on Advanced Computing & Communication Systems (ICACCS). doi:10.1109/icaccs.2019.8728456
[29]. AdewunmiTaiwo, A. and Ato Bart-Plange, A. Introduction of Smokeless Stove to Gari Producers at Koryire in the Yilokrobo Municipality of Ghana. International Journal of Advanced Engineering, Management and Science, vol. 2, no. 4, pp.163-169, 2016.
[30]. Ahmed, E. R., Islam, A., Zuqibeh, A., & Alabdullah, T. T. Y. Risks management in Islamic financial instruments. Advances in Environmental Biology, Vol. 8, no. 9, pp. 402-406, 2014.
[31]. Ahmed, E. R., Islam, M. A., Alabdullah, T. T. Y & bin Amran, A. Proposed the pricing model as an alternative Islamic benchmark. Benchmarking: An International Journal, Vol. 25, no. 8, pp. 2892-2912, 2018.
[32]. Alabdullah, T. T. Y., Ahmed, E. R., &Thottoli, M. M. Effect of Board Size and Duality on Corporate Social Responsibility: What has Improved in Corporate Governance in Asia?. Journal of Accounting Science, Vol. 3, no.2, pp. 121–135, 2019.
[33]. D. Mukherjee and B. V. R. Reddy, "Design and development of a novel MOSFET structure for reduction of reverse bias pn junction leakage current," International Journal of Intelligence and Sustainable Computing, vol. 1, no. 1, p. 32, 2020.
[34]. E. Malar and M. Gauthaam, "Wavelet analysis of EEG for the identification of alcoholics using probabilistic classifiers and neural networks," International Journal of Intelligence and Sustainable Computing, vol. 1, no. 1, p. 3, 2020.
[35]. Haldorai, A. Ramu, and S. Murugan, "Social Aware Cognitive Radio Networks," Social Network Analytics for Contemporary Business Organizations, pp. 188–202. doi:10.4018/978-1-5225-5097-6.ch010
[36]. J. Selvaraj and A. S. Mohammed, "Mutation-based PSO techniques for optimal location and parameter settings of STATCOM under generator contingency," International Journal of Intelligence and Sustainable Computing, vol. 1, no. 1, p. 53, 2020.
[37]. K. Jayasudha and M. G. Kabadi, "Soft tissues deformation and removal simulation modelling for virtual surgery," International Journal of Intelligence and Sustainable Computing, vol. 1, no. 1, p. 83, 2020.
[38]. M. Kasiselvanathan, V. Sangeetha, and A. Kalaiselvi, "Palm pattern recognition using scale invariant feature transform," International Journal of Intelligence and Sustainable Computing, vol. 1, no. 1, p. 44, 2020.
[39]. Mohmed Raffi, S., & P Lodha, D. A Review Paper on Hydrological Modelling and Climate Change in India. International Journal Of Advanced Engineering Research And Science, vol. 2, no. 1, pp. 40-41, 2015.
[40]. S. R. Mohamed and P. Raviraj, "Optimisation of multi-body fishbot undulatory swimming speed based on SOLEIL and BhT simulators," International Journal of Intelligence and Sustainable Computing, vol. 1, no. 1, p. 19, 2020.
[41]. S. S. Rao, "Semantic SPA framework for situational student-project allocation in education," International Journal of Intelligence and Sustainable Computing, vol. 1, no. 1, p. 69, 2020.
[42]. Ahmed, E. R., Alabdullah, T. T. Y., Amran, A., and Yahya, S. B. Indebtedness Theory and Shariah Boards: A Theoretical Approach. Global Business & Management Research, Vol. 10, no. 1, pp. 127-134, 2018.
[43]. Rajest, S. S., Suresh, D. The Deducible Teachings of Historiographic Metafiction of Modern Theories of Both Fiction and History. Eurasian Journal of Analytical Chemistry, vol. 13, no. 4, 2018 emEJAC191005.
[44]. K.B. Adanov, S. Suman Rajest, Mustagaliyeva Gulnara, Khairzhanova Akhmaral "A Short View on the Backdrop of American's Literature". Journal of Advanced Research in Dynamical and Control Systems, Vol. 11, No. 12, pp. 182-192, 2019.
[45]. Rao, A. N., Vijayapriya, P., Kowsalya, M., & Rajest, S. S. (2020). Computer Tools for Energy Systems. In International Conference on Communication, Computing and Electronics Systems .pp. 475-484), 2020 , Springer, Singapore.
[46]. Gupta J., Singla M.K., Nijhawan P., Ganguli S., Rajest S.S. An IoT-Based Controller Realization for PV System Monitoring and Control. In: Haldorai A., Ramu A., Khan S. (eds) Business Intelligence for Enterprise Internet of Things. EAI/Springer Innovations in Communication and Computing. Springer, Cham 2020.